Unhindered copper uptake of glutaraldehyde-polyethyleneimine coatings in an artificial seawater model system with adsorbed swollen polysaccharides and competing ligand EDTA

Simarpreet Kaur[a], Ivan M. Kempson[a], Johan B. Lindén[a,1], Mikael Larsson[a,b*] and Magnus Nydén[a,b]

[a]*Future Industries Institute, University of South Australia, Mawson Lakes, South Australia 5095, Australia.*

[b]*School of Energy and Resources, University College London, 220 Victoria Square, Adelaide, South Australia 5000, Australia*

Corresponding author: E-mail: larsson.mikael@gmail.com

Contact information:

SK; Phone number: +61 (0)469931624; Email: simarpreet_kaur@mymail.unisa.edu.au
IMK; Phone number: +61 (0)8 8302 3677; Email: ivan.kempson@unisa.edu.au
JBL; Phone number: +46105166066; Email: johan.linden@mymail.unisa.edu.au
ML; Phone number: +61 (0)883023493; Email: larsson.mikael@gmail.com
MN; Phone number: +61 (0)881109970; Email: m.nyden@ucl.ac.uk

[1]Current address: SP technical research institute of Sweden, Brinellgatan 4, 504 62 Borås, Sweden

Text: 5751

References: 647

Figures: 1312 (word equivalent)

Tables: 260 (word equivalent)

Unhindered copper uptake of glutaraldehyde-polyethyleneimine coatings in an artificial seawater model system with adsorbed swollen polysaccharides and competing ligand EDTA

ABSTRACT

Shortly after a surface is submerged in the sea, a conditioning film is generally formed by adsorption of organic molecules, such as polysaccharides. This could affect transport of molecules and ions between the seawater and the surface. Here an artificial seawater model system was developed to understand how adsorbed polysaccharides impact copper binding of glutaraldehyde-crosslinked polyethyleneimine coatings. Coating performance was also determined when competed against copper-chelating EDTA. The polysaccharide adsorption, copper binding and distribution was investigated using advanced analytical techniques, including depth-resolved time-of-flight secondary ion mass spectroscopy, grazing incidence X-ray absorption near edge spectroscopy, quartz crystal microbalance with dissipation monitoring and X-ray photoelectron spectroscopy. In artificial seawater the polysaccharides adsorbed in a swollen state that copper readily penetrated and the glutaraldehyde-polyethyleneimine coatings outcompeted EDTA for copper binding. Furthermore, depth distribution of copper species was determined with nanometer precision. The results are highly relevant for copper-binding and releasing materials in seawater.

Keywords: antifouling; biocidal metals; copper chelation; kinetics; polyethyleneimine; selective binding

Introduction

Marine biofouling is a "billion dollar problem" (Schultz et al. 2011). The most efficient of the antifouling coatings have traditionally relied on release of biocidal metals that have ultimately led to significant pollution and associated detriment to the environment (Trentin et al. 2001).

Many of such products have been banned and there is currently no equally effective alternative available for widespread use (Del Grosso et al. 2016). In today's coatings, copper is widely used as the most effective broad-spectrum biocide (Finnie and Williams 2010, Del Grosso et al. 2016). However, concerns are being raised regarding the impact of released copper on the marine environment in protected waters such as marinas and harbours (Ohlauson and Blanck 2014) and its use may be restricted in the near future (Townsin 2003, Srinivasan and Swain 2007). Contemporary environmentally friendly solutions rely on shear forces produced with a vessels' motion (Lejars et al. 2012), while in fact, the most severe biofouling actually occurs when vessels are stationary (Lindholdt et al. 2015). As such, these technologies are not highly active when needed the most and become defunct for static marine structures (Laidlaw 1952, Brady 2001).

It has been shown that glutaraldehyde (GA)-crosslinked polyethyleneimine (PEI) coatings selectively and effectively accumulate copper from artificial (Lindén et al. 2014, Lindén et al. 2016) and real seawater (Lindén et al. 2015), indicating potential for advanced marine applications that harvest copper for sensing (Yuan et al. 2013, Zhang et al. 2013), remediation (Goon et al. 2010, Bertagnolli et al. 2015) and antifouling coatings. Of particular interest to the present authors is to develop a polymer based antifouling coating capable of cycling between copper uptake from seawater and copper release for biocidal action, ie no copper is introduced to the environment and has an antifouling functionality well suited to vessels at port and stationary objects and structures.

Biofouling instigates with the adsorption of a polysaccharide-rich organic film that forms on surfaces within a few minutes after submersion in seawater (Yebra et al. 2004). This organic film enables adherence and growth of marine organisms while simultaneously repressing

biocidal activity, leading to possible failure of the antifouling functionality (Chambers et al. 2006). The authors of this paper have demonstrated an exceptional copper uptake from artificial seawater for recently developed nano-thin GA–PEI coatings (Lindén et al. 2014) which served as the first milestone towards development of the copper-cycling antifouling coatings discussed above. In real seawater, copper binding efficacy and kinetics were slightly reduced, which was hypothesized to be due to the formation of such an organic film (Lindén et al. 2015). Here advanced characterization techniques were used to investigate if an adsorbed conditioning layer in the form of polysaccharides impacted the copper uptake and to provide the most in-depth insight into copper absorption into such coatings currently achieved. The capacity of the seawater relevant carrageenan, sodium alginate and agarose polysaccharides (Renn 1997) to adsorb to and penetrate into such coatings was assessed, followed by demonstration of how the copper is interred and associated with nanometer-scale precision with respect to the depth in the coating. This acts as a highly sophisticated elucidation as to how polysaccharide adsorption initiates with respect to the function of such antifouling coatings. It further reveals how copper is transferred and incorporated under semi-realistic model marine conditions in context of developing new marine technologies involving transport and binding of copper. The chemical structures of polysaccharides used in this study are shown in Figure 1.

<center>**<FIGURE 1 HERE>**</center>

Materials and methods

Materials

Branched polyethyleneimine (PEI, 50 wt% in H_2O, Mn ~ 60,000 and MW ~ 750,000), glutaraldehyde (GA, 25 wt% in H_2O), sea salts, ethylenediaminetetraacetic acid (EDTA), carrageenan from sea weed (non-gelling mixture of lambda and kappa carrageenans), alginic

acid sodium salt from brown algae (medium viscosity) and agarose sodium salt were purchased

from Sigma Aldrich (Australia) and used without further purification. Copper(II) sulphate

pentahydrate was purchased from Chem-Supply Pty Ltd and was used to make all copper-

containing solutions. Ultrapure water with a resistivity of 18.2 MΩ cm was obtained using a

Milli-Q® Advantage A10® water purification system. Artificial seawater was prepared by

dissolving 38 g of sea salts per litre of Milli-Q water and the pH was determined to 8.1-8.3 using

an ION 700 meter equipped with a pH electrode (Eutech instruments, Singapore). The

composition of the artificial seawater is specified in Table S1.

Preparation of GA–PEI coatings

Glutaraldehyde-crosslinked PEI (GA–PEI) coatings were prepared on cut 1 x 1 cm silicon wafers

or gold-QCM sensors (Q-sense, Biolin Scientific) following the method described by Lindén

et.al. (Lindén et al. 2014). Silicon wafers were cut manually with a diamond cutter into 1 x 1 cm

samples. The samples were washed by sonication with 2% RBS 35 detergent solution (Thermo

Scientific) for 15 minutes, rinsed with Milli-Q water, sonicated in Milli-Q water for 15 minutes,

rinsed with Milli-Q water and stored in ethanol. Prior to the use, samples were rinsed with

ethanol and dried under N_2 gas. Following this, the GA–PEI coatings were prepared by spin

coating silicon wafer samples with PEI from 0.05% solution in ethanol and immersing in 0.5%

GA solution for crosslinking. The samples were then re-immersed in PEI solution to get rid of

the excess GA before washing and drying under N_2 gas.

Preparation of polysaccharide solutions

Solutions of Carrageenan, alginate and agarose were prepared to 0.1 wt% in Milli-Q water followed by dilution in artificial sea water to 0.001 wt%, 0.005 wt% and 0.025 wt%. Samples were assessed as dissolved or non-dissolved through visual inspection.

Quartz crystal microbalance with dissipation (QCM-D) analysis

The adsorption of polysaccharides in artificial seawater onto GA–PEI coatings and the stability of the formed layers were investigated using QCM-D (E4, Q-sense, Sweden) with gold coated QCM-sensors. All the solutions were degassed for 5 minutes using ultrasonic bath (LGO model 120W-CHM series-29). The solutions were run at the rate of 0.1 mL/min over the sensors. The adsorption and viscoelastic changes in the coating and adsorbed layer were monitored through the change in resonance frequency (Δf) and dissipation (ΔD), respectively. Measurements were performed in quadruplicate. The hydrated thickness of the adsorbed polysaccharide layer was modelled using Kelvin-Voigt model for a single layer system with power-law frequency dependence of storage shear modulus and viscosity. The fitting of the measured changes in resonance frequency (Δf) and dissipation (ΔD) following the adsorption of carrageenan and alginate was performed using Q-tools software 3. The parameters used as fixed were the fluid density (1.0 g/cm^3) and fluid viscosity (0.001 kg/sm). The layer densities used in the final model was acquired by iterations starting with the dry densities of the polysaccharides (1.37 g/cm^3 for carrageenan and 1.6 g/cm^3 for alginate) and estimating the densities of swollen layers based volume fraction weighted densities of the polysaccharides and water. Other layer parameters to be fitted were bound within the following ranges: viscosity (0.5 g/sm - 10 g/sm), shear modulus (0.01 - 1000 MPa), thickness (1 – 100nm). The fundamental frequency was set equal to 4.95

MHz and the measured QCM-D data for quadruplet of samples was modelled at 5 different harmonics- 3, 5, 7, 9, and 11. Descending incremental fitting was used.

Preparation of samples for copper uptake studies

For copper uptake studies GA–PEI coatings on 1 x 1 cm silicon wafers were submerged in artificial seawater solutions of 0.001 wt% carrageenan or sodium alginate for 9 hours. Subsequently the samples were thoroughly rinsed with Milli-Q water followed by drying with N_2 gas. To ensure successful sample preparation and the presence of a stable polysaccharide layer the dry thicknesses of the samples were determined after each preparation step using a variable angle spectroscopic ellipsometer (VASE®) and WVASE32® software (J.A. Woollam Co., Inc.).

Atomic force microscopy measurements (AFM)

Surface morphology of GA-crosslinked PEI with and without adsorbed polysaccharides was determined in air using ScanAsyst on a Nanoscope MultiMode 8 AFM with a Nanoscope V controller (Bruker). The data was processed using WSxM v5.0 Develop 8.0 software from WSxM solutions.

Copper uptake and removal

The copper uptake of coatings with an adsorbed polysaccharide layer was investigated by submerging samples in artificial seawater spiked with 200 ppb of copper from copper(II) sulphate pentahydrate. At predetermined times samples were extracted, rinsed with Milli-Q water, dried with N_2 gas and analysed for copper content using XPS. The XPS measurements were undertaken using monochromatized Al Kα-rays (1486.7 eV) at a power of 225W on a Kratos Axis-Ultra spectrometer (160 eV analyser pass energy for survey scans, 20 eV for high-

resolution scans) and an analysis spot size of ~ 300 x 700 μm. The data processing (peak fitting)

and quantification was performed with the casa XPS software, using a Tougard type background

subtraction. Two samples were analysed for each time-point and the elemental composition of a

sample was determined as the average of measurements at two different spots. The atom

percentage of copper was used to estimate the copper content of the coatings.

To determine the efficacy for copper uptake in the presence of polysaccharides and/or

competing ligands, GA–PEI was prepared on DE particles as previously reported (Lindén et al.

2016). The GA–PEI–DE particles were dispersed at 2.5 mg/ml in 40 ml of pure artificial

seawater or with 0.001 wt% of carrageenan or alginate, 0.001% of each and/or 92 mg/l EDTA

for 9 hours. Polysaccharide solutions had been prepared from concentrated stock-solutions in

Milli-Q water. EDTA solutions had been prepared by adding 92 ppm of EDTA to artificial

seawater (partially dissolved; pH = 6.5 – 6.6). Subsequently the pH was raised to 8.1 – 8.2 using

~1 M NaOH and the solution was heated to 60 $^\circ$C and mixed until EDTA was completely

dissolved. After mixing particles with the solutions they were spiked with 200 or 90 ppb copper

followed by agitation at room temperature overnight. The dispersions and controls without

particles were centrifuged at 4000 rpm for 5 minutes and supernatant was collected. The

supernatant was collected, 3-6 drops of TraceSELECT grade HNO_3 (Sigma-Aldrich) were added

and copper concentration was determined from three readings using a Perkin Elemer ICP-OES

Optima 7300DV. All results were processed with MSF (Multicomponent Spectral Fitting).

Standards were prepared in 1% HNO_3. To determine if EDTA was removed from solution in the

process, the UV-Vis signal of EDTA-Cu complexes was used. Samples were extracted before

and after the removal of copper by the GA–PEI–DE and copper sulfate was added to achieve the

same molar copper concentration as the initial molar concentration of EDTA (0.31 mM). The

UV-Vis spectra of the EDTA-Cu complexes were recorded with a Varian Cary 300 Bio UV/Vis spectrometer using a quartz cuvette. Pure artificial seawater, artificial seawater containing 0.31 mM EDTA without the added copper and Milli-Q water containing 0.31 mM of copper sulfate (since copper sulfate is not fully soluble at this concentration in the artificial seawater) were included as controls.

Time-of-flight secondary ion mass spectroscopy (ToF-SIMS)

ToF-SIMS was utilized to elucidate the spatial elemental and molecular composition of the coatings with adsorbed polysaccharide layer after 216 hours of copper uptake. Experiments were performed under a vacuum of 5×10^{-6} Pa or better using a Physical Electronics Inc. PHI TRIFT V nanoTOF instrument equipped with a pulsed liquid metal Au primary ion gun (LMIG), operating at 30 keV energy. Depth profiling was performed using an Ionoptika 20 keV $C60^{+}$ source of 500 x 500 micron raster. "Bunched" Au_1 instrumental settings were used to optimise mass resolution for the collection of positive and negative SIMS for analysis within the sputter 'crater' using a 100 x 100 micron raster. Data were processed and analysed in WinCadence N1.8.1 software.

Grazing incidence X-ray absorption near edge spectroscopy (GI-XANES).

Data was collected by measuring X-Ray Fluorescence emission in a grazing incidence mode at the International Atomic Energy XRF beamline in the Elettra Synchrotron, Trieste, Italy. The source is a bending magnet providing a broad excitation energy range (2-14 keV) provided by a double crystal monochromator of a resolving power $1.4 \ 10^{-4}$. The beam is shaped to a 250 x 100 μm beamsize (hor x ver) with slits at ~ 23 m from the source, with an angular divergence of 0.15 mrad and a transmitted flux of about $5 \ 10^{9}$ ph/s (at 5500 eV, machine mode 2 GeV). Regions of scans presented were conducted with 0.5 eV increments from 8,970 eV to 9,030 eV

encompassing the Cu-K absorption edge. Incidence angles of 50% and 90% of the critical angle, as determined for our system, were used to probe differences in copper association as a function of depth. 50% of the critical angle was the most surface sensitive arrangement while 90% of the critical angle probed deeper into the sample.

X-ray absorption spectroscopy (XAS)

XANES was conducted at the XAS beamline at the Australian Synchrotron using a 1.9T Wiggler insertion device and a Si (111) monochromator. Nominal specifications gave an energy resolution of 1.5×10^{-4}, beam size of 250 x 250 microns and a flux of 10^{10} to 10^{12} ph/s. Absorption of the incident X-ray beam was monitored by fluorescence with a 100 element germanium detector perpendicular to the incident beam. Cryogenic temperatures were maintained between 5-10 K for the duration of analysis. XANES was performed over the Cu-K edge (8,979 eV) with the pre-edge region acquired in 10 eV steps before using 0.25 eV steps from 8,975 to 9,012.5 eV followed by 0.06 steps in K out to 6 K.

Results and discussion

Preparation of polysaccharide solutions

To establish the model polysaccharide-containing artificial seawater, solutions were prepared at different concentrations (0.025 – 0.001 wt%) and the dissolution of the polysaccharides was examined by visual inspection. Out of carrageenan, sodium alginate and agarose considered, only the former two polysaccharides were found to be entirely soluble in artificial seawater at pH 8, even for concentrations as low as 0.001 wt% (Table 1). Based on the results, carrageenan and

sodium alginate were selected to further investigate the impact of polysaccharide adsorption on the copper uptake of the GA-crosslinked PEI-based coatings.

\<TABLE 1 HERE\>

Characterization of polysaccharide adsorption, stability and thickness of the formed films

The adsorption of polysaccharides onto the GA–PEI coatings was investigated using QCM-D technique. GA-crosslinked PEI coatings with a thickness of about 9 nm were prepared on gold QCM-sensors, by the procedure previously described (Lindén et al. 2014). During the experiment, the GA–PEI coatings were exposed to Milli-Q water and artificial seawater to establish the baselines of the material in those solvents. Subsequently artificial seawater containing carrageenan or alginate (0.001 wt%) was introduced. Samples were then washed by again introducing Milli-Q water and artificial seawater. Finally, the samples were exposed to artificial seawater containing 200 ppb copper. Adsorption of carrageenan and alginate onto the GA–PEI coating was confirmed by monitoring the films' mass, indicated by a decrease in frequency (f), as a function of time with Quartz Crystal Microbalance with Dissipation (QCM-D) (Figure 2, Region I). Carrageenan adsorbed significantly faster than alginate, reaching close to equilibrium in 3 hours and 15 minutes. Alginate on the other hand required 13 hours to reach a comparable relative shift in frequency. The dissipation value, D, was quite different between the polysaccharides (15 versus 22) however both indicated swollen, or rough, structures. Based on the frequency measurements, rinsing with Milli-Q water and artificial seawater consecutively proved that the polysaccharide layers were stably adsorbed (Figure 2, Region II). Simultaneously, the dissipation measurements indicated that Milli-Q water collapsed the

polysaccharide structure while artificial seawater resulted in a swollen material with viscoelastic properties. It could be seen that upon re-application of artificial seawater the *f*-values further decreased to values 45 Hz and 65 Hz lower than in artificial seawater prior to polysaccharide adsorption for carrageenan and alginate, respectively. The D-values on the other hand increased to values about 5 and 15 units larger than before the adsorption for carrageenan and alginate, respectively. This behaviour can be explained by that in artificial seawater the interactions between the negatively charged polysaccharides and the positively charged GA–PEI was screened by the salt ions, allowing for swelling of the adsorbed layer, while in Milli-Q water there were no ions to interfere with the electrostatic interactions. A 200 ppb copper solution was then introduced and indeed an increase in mass of the sample was observed, indicating an influx of copper that changed the mass and viscoelastic nature of the film (Figure 2, Region III). Conclusions on the actual mass of copper taken up by the system from the QCM-D data is prevented since the mass change could be from both the actual copper ions and from influx of other ions and water into the system. The complexity is highlighted by that the dissipation increased in presence of copper, whereas the crosslinking effect of a coordinating metal would be expected to result in a more rigid system (Andersson et al. 2011).

<FIGURE 2 HERE>

Given the viscoelastic character of the adsorbed layers the hydrated thickness was modelled by an extended viscoelastic Voigt model for a single layer system. The *f* and D values from the modelling were in good agreement with the measured QCM-D data (Table S2) and the modelled viscosity and shear modulus presented values and behaviour of physical relevance (Figure S1).

Furthermore, the Sauerbrey equation was borderline valid for the solid-like layer of carrageenan in Milli-Q water ($\Delta D/(-\Delta f/\text{n}) < 4 \times 10^{-7}$) (Reviakine et al. 2011) and resulted in an estimated thickness of 3 ± 0.7 nm, in good agreement with the thickness of 2.4 ± 0.5 nm from the viscoelastic modelling. It was thus concluded that the Voigt extended viscoelastic model could be used to describe the system. The model suggested the thickness of the carrageenan layer to be about 2.4 nm in Milli-Q water and 21 nm in artificial seawater. For alginate the thickness was about 13 nm in Milli-Q water and 38 nm in artificial seawater (Table S3). In other words, the hydrated layer thickness was larger for alginate than for carrageenan, both in Milli-Q water and artificial seawater. The larger dissipation values for alginate, compared to carrageenan, suggested that alginate presented a more swollen layer.

Taken together with the hydrated thicknesses from the QCM-D modelling, the results strongly indicate that the polysaccharide layers were somewhat swollen in Milli-Q water and highly swollen in artificial seawater, with alginate being more swollen than carrageenan. These are highly interesting results, suggesting that under the ionic composition of seawater, these polysaccharide films conform to a permeable structure that can pass ions or small molecules from solution to the underlying substrate and vice-versa.

To further confirm swelling of the films, ellipsometry measurements were conducted at each step of the preparation and indicated that the dry layer thickness of adsorbed alginate was about 2 nm, while that of carrageenan was about 3 nm (Figure 3). By combining the ellipsometry and the QCM-D results the volume expansion of the polysaccharide layers in artificial seawater was estimated to 19 and 7 for alginate and carrageenan, respectively.

<FIGURE 3 HERE>

Morphology of the adsorbed polysaccharide films

Surface topography of the adsorbed carrageenan and alginate layers on the GA–PEI coatings was examined by AFM on dried samples. It was confirmed that polysaccharide layers covered the GA–PEI coatings as the small pinholes that were present in the bare GA–PEI coating disappeared after the polysaccharide adsorption (Figure 4). Carrageenan adsorbed as a rather smooth layer with only some larger particle-like aggregates (Figure 4b). Alginate presented numerous small but distinct structures as well as larger aggregates resembling thread-like bundles (Figure 4c). These observations were reinforced by the respective height histograms with the distributions for carrageenan (Figure 4b) and alginate (Figure 4c) covered surfaces presenting a tail towards higher structures compared to the bare GA–PEI surface (Figure 4a) and with this tail being longer and more pronounced for alginate.

<FIGURE 4 HERE>

Distribution of copper into GA–PEI coatings with adsorbed polysaccharides

XPS analysis of copper uptake kinetics

Having established the stable adsorption of the polysaccharides on the GA–PEI coatings, the impact of such layers on copper uptake kinetics and equilibrium was investigated by analysing the atom% copper by XPS. GA–PEI coatings with a thickness of about 9 nm (Figure 3) were prepared on silicon 1 x 1 cm silicon wafter substrates. Subsequently, the copper uptake in excess of artificial seawater containing 200 ppb copper (from copper(II) sulphate pentahydrate) was evaluated over 72 h for samples with and without an adsorbed layer of carrageenan or alginate. A copper(II) salt was used as Cu^{2+} is the major oxidation state found in the sea (Byrne 2007). The experimental time was chosen so that equilibrium copper uptake would be achieved if unaffected

by the adsorbed polysaccharides (Lindén et al. 2014). At the final time point the total amount of copper in the coatings was similar (about 1.3 atom%), with or without adsorbed polysaccharides (Figure 5a). Interestingly, for coatings with adsorbed carrageenan, the atom% of copper was consistently lower up until the last time point compared to coatings with adsorbed alginate or with no adsorbed polysaccharide. In contrast, the copper-to-nitrogen ratio was similar (Figure 5b), or even hinted to be somewhat higher at later times compared to the sample without polysaccharides. An explanation for these observations could be the surface-sensitive nature of XPS and copper-distribution in the carrageenan sample. In a simplified theoretic scenario, the contribution of photoelectrons from a certain depth (z) to the total XPS signal decreases exponentially according to (Jablonski 1994):

$$\emptyset(z) = \frac{1}{\lambda \cos \alpha} \, exp\left(-\frac{z}{\lambda \cos \alpha}\right) \tag{1}$$

where λ is the inelastic mean free path (IMFP) and α is the detection angle with respect to the surface normal. For polymer materials the IMFP is around 2-3 nm for the energies used in this study (Cumpson 2001). By integration of Eq. 1 and assuming an IMFP of 3 nm, the theoretical fraction of the XPS signal coming from the top 3 nm of the sample is 63%, the fraction coming from the depth 3-5 nm is 23% and from deeper than 5 nm 14%. Although real values may differ from theory, the XPS signal is weighted towards elements in the upper most part of the sample, ie the polysaccharide layer and immediately underlying regions. Thus, a sample with an adsorbed dense polysaccharide layer (no nitrogen) with a copper concentration lower than the underlying nitrogen-containing coating could present a decreased atom% of copper and an increased copper-to-nitrogen ratio compared to a sample without the adsorbed polysaccharide layer. Thus the results loosely suggest a small but relevant amount of copper in the carrageenan

layer. For alginate this behavior was not observed and the atom% of copper and copper-to-nitrogen ratio were similar relative to the coating without adsorbed polysaccharides. The large variations in data and the fact that alginate adsorbed in elevated patches with low total surface coverage, as revealed by the AFM analysis discussed above, prevent detailed discussions on potential copper-distribution throughout the thickness of the coating based on the XPS data for the samples with adsorbed alginate.

With regard to kinetics, the rate of copper-uptake was similar for all conditions, but possibly marginally slower with adsorbed carrageenan. As hypothesized from the QCM-D and ellipsometry data, these results prove that copper ions can readily diffuse through the highly swollen polysaccharide structures.

<FIGURE 5 HERE>

ToF-SIMS analysis of copper and polysaccharide distribution

Design of advanced functional coatings for the envisaged applications requires further fundamental understanding of how copper is associated and distributed in such coatings. Thorough analysis is highly challenging due to low absolute quantities and nanometer-scale thickness. In approaching this challenge, attempts were made to produce depth profiles of copper distribution through the coatings utilising ToF-SIMS. Subsequently, 3-dimensional reconstructions of the chemical composition of the polysaccharide layer (represented by $C_3H_5^+$), GA–PEI coating ($C_2H_5N^+$) and the underlying Si substrate (Si^+) along with the general copper (Cu^+) distribution were produced (Figure 6). Furthermore, the mass spectrometric fragments

indicative of copper associations at different depths were also identified. Thus, not only was the

copper distribution identified, but also its chemical association in the different layers. A Cu_2OH^+

was present at the surface which appeared to be more significant (approximately 2.5 times the

peak integral) for the carrageenan coating compared to alginate. This was determined by the total

absolute counts for this mass fragment and is indicated by the greater abundance of the pink

colour designated in the 3D reconstruction in Figure 6. A nitrogen association in the GA–PEI

coating was identified by the presence of a Cu_2CN^+ species ejected in the sputtering process.

<p align="center">**<FIGURE 6 HERE>**</p>

XAS analysis of copper speciation

To further explore these observations of differing copper association with depth and

polysaccharide, the same systems were analysed over the Cu K-edge with X-ray Absorption

Spectroscopy (XAS) in a grazing incidence configuration at the International Atomic Energy

Agency's X-ray fluorescence beamline at the Elettra synchrotron, Italy. The surfaces were

probed at 50% and 95% of the angle of total reflection which provides characterization of copper

at the very near surface and slight sub-surface respectively. Copper was only detected in a form

consistent with a Schiff-base complex (Lindén et al. 2015) for the alginate sample and the sub-

surface carrageenan sample (Figure 7). Moving to a more surface sensitive geometry for

carrageenan led to the introduction of a shoulder in the spectrum consistent with a hydroxide

species (Figure S2).

Collectively, the XPS, ToF-SIMS and grazing incidence XAS are all consistent in how

copper is perceived to be distributed and associated in the nano-scale thin films and coatings. In

the very top layer, copper appears to be to be associated with the polysaccharides in a copper

hydroxide state, with the abundance being greater for coatings with adsorbed carrageenan than with adsorbed alginate. More importantly, copper penetrated through the adsorbed polysaccharide layer into the underlying GA–PEI coating and bound in a state resembling a Cu^{2+}-Schiff-base complex.

<FIGURE 7 HERE>

Copper removal by GA–PEI–DE particles in the presence of polysaccharides and chelating ligands

In a real marine environment, competing copper-binding ligands will be present in addition to adsorbing polysaccharides. Therefore, in a final test of the GA–PEI coatings in a highly demanding model marine environment, polysaccharide coated GA–PEI layers adsorbed on silica diatomaceous earth particles, prepared as previously described (Lindén et al. 2016), were competed against the known copper chelator EDTA (Maketon et al. 2008). GA–PEI–DE particles were suspended at 2.5 mg/ml (resulting in about 150 ppm of the copper-binding GA–PEI material) in artificial seawater containing either 0.001% of alginate or carrageenan, 92 ppm EDTA as a competing ligand or a combination of all. It is worth noting that at the used concentrations of GA–PEI–DE and EDTA the two materials were estimated to present roughly the same number of copper-binding sites.

Polysaccharides were given 9 hours for adsorption before adding copper at 90 or 200 ppb. Samples were stirred over night before particles were pelleted by centrifugation and the copper concentration in the supernatant determined by inductively coupled plasma optical emission spectrometry (ICP-OES). The results revealed that the GA–PEI–DE particles

effectively removed copper to ≤ 10 ppb (the detection limit of the ICP-OES) for artificial seawater and all investigated combinations of polysaccharides and EDTA (Table 2).

<TABLE 2 HERE>

For controls without particles, no decrease was seen in copper concentration from the treatment and it was further confirmed that the presence of polysaccharides in themselves did not result in copper removal (Figure S3).

The result that GA–PEI material can outcompete excess EDTA for copper binding has previously been reported for the less complex solution of synthetic electroplating rinse water ($CuSO_4$ and H_2SO_4) with pH set to 5-6 (Revathi et al. 2015). It has also been reported that PEI can remove EDTA and copper-EDTA complexes from solution through electrostatic interactions (Maketon et al. 2008), which could result in copper removal without the EDTA-copper bond being broken. Such electrostatic interactions are weak compared to the metal-chelation bond and were not expected to result in EDTA or EDTA-copper removal in the high ionic-strength conditions of artificial seawater. UV-vis analysis before and after the copper-uptake procedure indeed confirmed that EDTA was not removed by the GA–PEI–DE (Figure S4). It was therefore concluded that the copper removal was by GA–PEI–DE outcompeting EDTA for copper-binding. To our knowledge this is the first report on the impact of EDTA on copper-binding resins in seawater-relevant solutions. We also believe that this is the first report that studies the impact of surface-adsorbed polysaccharides on the copper-binding performance of resins in a seawater-relevant environment.

Conclusions

We have demonstrated that nano-thin coatings based on glutaraldehyde-crosslinked (GA-crosslinked) polyethyleneimine (PEI) could effectively take up copper from concentrations relevant to contaminated harbours, and that the uptake performance was unaffected by adsorption of alginate and/or carrageenan or by a copper-competing ligand in the solution (EDTA). Furthermore, we have thoroughly elucidated with nanoscale depth resolution where and how copper distributes and associates in these multi-layer films. The findings revealed that in seawater, alginate and carrageenan adsorbed in a swollen state through which copper can readily diffuse and that the GA-PEI coatings outcompeted the strong copper-chelator EDTA. The results further strengthen the potential of the GA-PEI material to scavenge copper from the sea for the long-term goal of making a new antifouling coating with no net release of biocides.

Acknowledgements

Government; and Peter Kappen and Chris Glover for the bulk XAS measurements undertaken on

the X-ray Absorption Spectroscopy beamline at the Australian Synchrotron, Victoria, Australia

References

Andersson M, Hansson Ö, Öhrström L, Idström A, Nydén M. 2011. Vinylimidazole copolymers: coordination chemistry, solubility, and cross-linking as function of Cu^{2+} and Zn^{2+} complexation. Colloid Polym. Sci. 289:1361-1372.

Bertagnolli C, Grishin A, Vincent T, Guibal E. 2015. Synthesis and Application of a Novel Sorbent (Tannic Acid-Grafted-Polyethyleneimine Encapsulated in Alginate Beads) for Heavy Metal Removal. Sep Sci Technol. 50:2897-2906.

Brady RF. 2001. A fracture mechanical analysis of fouling release from nontoxic antifouling coatings. Prog Org Coat. 43:188-192.

Byrne RH. 2002. Speciation in Seawater. In: Ure AM, Davidson CM, editors. Chemical Speciation in the Environment. Oxford: Blackwell Science Ltd.

2007, pp. 322-357.

Chambers LD, Stokes KR, Walsh FC, Wood RJ. 2006. Modern approaches to marine antifouling coatings. Surf Coat Technol. 201:3642-3652.

Cumpson PJ. 2001. Estimation of inelastic mean free paths for polymers and other organic materials: use of quatitative structure-property relationships. Surf. Interface Anal. 31:23-34.

Del Grosso CA, McCarthy TW, Clark CL, Cloud JL, Wilker JJ. 2016. Managing Redox Chemistry to Deter Marine Biological Adhesion. Chem Mater. 28: 6791-6796.

Finnie AA, Williams DN. 2010. Paint and coatings technology for the control of marine fouling. Biofouling. 185-201.

Goon IY, Zhang C, Lim M, Gooding JJ, Amal R. 2010. Controlled fabrication of polyethylenimine-functionalized magnetic nanoparticles for the sequestration and quantification of free Cu^{2+}. Langmuir. 26:12247-12252.

Jablonski A. 1994. Escape depth of photoelectrons. Surface and interface analysis. 21:758-763.

Laidlaw F. 1952. The history of the prevention of fouling. Woods Hole Marine Oceano Inst, ed Fouling and its prevention Annapolis, US Naval Inst. 211-223.

Lejars M, Margaillan A, Bressy C. 2012. Fouling Release Coatings: A Nontoxic Alternative to Biocidal Antifouling Coatings. Chem Rev. 112:4347-4390.

Lindén JB, Larsson M, Coad BR, Skinner WM, Nydén M. 2014. Polyethyleneimine for copper absorption: kinetics, selectivity and efficiency in artificial seawater. RSC Adv. 4:25063-25066.

Lindén JB, Larsson M, Kaur S, Skinner WM, Miklavcic SJ, Nann T, Kempson IM, Nydén M. 2015. Polyethyleneimine for copper absorption II: kinetics, selectivity and efficiency from seawater. RSC Adv. 5:51883-51890.

Lindén JB, Larsson M, Kaur S, Nosrati A, Nydén M. 2016. Glutaraldehyde□crosslinking for improved copper absorption selectivity and chemical stability of polyethyleneimine coatings. J Appl Polym Sci. 133:43954.

Lindholdt A, Dam-Johansen K, Olsen SM, Yebra DM, Kiil S. 2015. Effects of biofouling development on drag forces of hull coatings for ocean-going ships: a review. J Coat Technol Res. 12:415-444.

Maketon W, Zenner CZ, Ogden KL. 2008. Removal efficiency and binding mechanisms of copper and copper-EDTA complexes using polyethyleneimine. Environ. Sci. Technol. 42:2124-2129.

Ohlauson C, Blanck H. 2014. A comparison of toxicant-induced succession for five antifouling compounds on marine periphyton in SWIFT microcosms. Biofouling. 30:41-50.

Renn D. 1997. Biotechnology and the red seaweed polysaccharide industry: status, needs and prospects. Trends Biotechnol. 15:9-14.

Revathi M, Ahmed Basha C, Velan M. 2015. Removal of copper (II) ions from synthetic electroplating rinse water using polyethyleneimine modified ion-exchange resin. Desalination Water Treat. 57:20350-20367.

Reviakine I, Johannsmann D, Richter RP. 2011. Hearing what you cannot see and visualizing what you hear: interpreting quartz crystal microbalance data from solvated interfaces. Anal Chem. 83:8838-8848.

Schultz M, Bendick J, Holm E, Hertel W. 2011. Economic impact of biofouling on a naval surface ship. Biofouling. 27:87-98.

Srinivasan M, Swain GW. 2007. Managing the use of copper-based antifouling paints. Environ manage. 39:423-441.

Townsin R. 2003. The ship hull fouling penalty. Biofouling. 19:9-15.

Trentin I, Romairone V, Marcenaro G, De Carolis G. 2001. Quick test methods for marine antifouling paints. Prog Org Coat. 42:15-19.

Yebra DM, Kiil S, Dam-Johansen K. 2004. Antifouling technology—past, present and future steps towards efficient and environmentally friendly antifouling coatings. Prog Org Coat. 50:75-104.

Yuan Z, Cai N, Du Y, He Y, Yeung ES. 2013. Sensitive and selective detection of copper ions with highly stable polyethyleneimine-protected silver nanoclusters. Anal Chem. 86:419-426.

Zhang N, Qu F, Luo HQ, Li NB. 2013. Sensitive signal-on fluorescent sensing for copper ions based on the polyethyleneimine-capped silver nanoclusters–cysteine system. Anal Chim Acta. 791:46-50.

Figure legends

Figure 1. Chemical structures of various polysaccharides considered in this study: (a) Lambda carrageenan; (b) Sodium alginate; and (c) Agarose.

Figure 2. Representative QCM-D sensograms for adsorption and stability of (a) Carrageenan and (b) Alginate adsorbed onto the GA–PEI coatings from artificial seawater containing 0.001 wt% of the polysaccharide. Change in frequency (black) is given on the left Y-axis and dissipation (grey) is given on the right Y-axis. The vertical blue lines refer to the change of solution with 1 indicating Milli-Q water, 2 indicating artificial seawater (AS) and 3 indicating either (a) 0.001% carrageenan or (b) 0.001% alginate in artificial seawater. Region I includes establishment of baseline for GA–PEI in Milli-Q water 1 and artificial seawater 2, with subsequent adsorption of the polysaccharide (a) carrageenan and (b) alginate from artificial seawater 3, respectively. In Region II the stability of the adsorbed films was investigated upon reapplication of solutions 1 and 2. This was followed by copper uptake from 200 ppb in AS in Region III. The fifth overtones are graphed (F5 & D5).

Figure 3. Average thickness at different stages of the preparation process for GA–PEI coatings with an adsorbed layer of polysaccharide. Error bars indicate one standard deviation (n=54 and 22 for coatings with and without adsorbed polysaccharides, respectively.

Figure 4. The top row presents AFM height images (10 x 10 μm^2) of (a) PEI crosslinked with glutaraldehyde (GA–PEI) (b) Carrageenan on GA–PEI (c) Alginate on GA–PEI on a silicon wafer substrate. The small pinholes visible in (a) GA–PEI disappear after the adsorption of (b) Carrageenan or (c) Alginate The bottom row presents relative height histograms for the AFM topographic images respectively. Both (b) carrageenan and (9c) alginate covered surfaces presented a tail in the distribution towards higher structures, compared to bare (a) GA–PEI, with the tail being the most pronounced for alginate.

Figure 5. Graphs showing (a) Atom% copper (Cu) and (b) Copper-to-nitrogen (Cu/N) ratio for GA–PEI coatings without adsorbed polysaccharides (●; circles), with adsorbed carrageenan (■; squares) and with adsorbed alginate (▲; triangles) after different immersion times in artificial seawater containing 200 ppb copper. Error bars indicate ± min/max (n = 2).
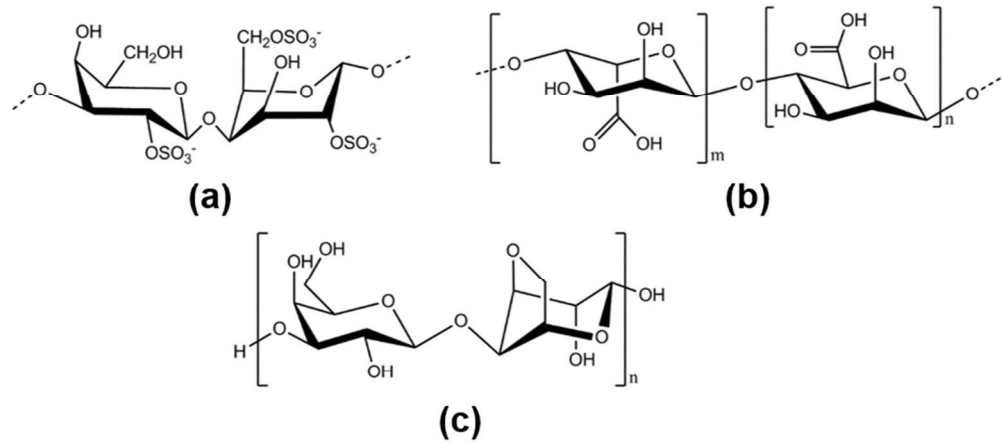
Figure 6. Tof- SIMS depth profile through GA–PEI coatings adsorbed with (a) Carrageenan or (b) Alginate from 0.001% solution in artificial seawater. To the right are the corresponding 3D reconstruction of the Tof-SIMS depth profile presenting polysaccharide through C3H5+ fragment (pink) on a silicon substrate (blue) showing copper (red).

Figure 7. Cu K-edge XANES spectra for copper; in GA–PEI adsorbed with carrageenan and GA–PEI adsorbed with alginate.

Table headings

Table 1. Solubility of carrageenan, sodium alginate and agarose at three different concentrations in artificial seawater (pH 8). "+" indicates fully soluble and "-"indicates not fully soluble, as determined by visual inspection.

Table 2. Copper concentration after copper removal from artificial seawater by GA–PEI -DE particles. Initial copper concentration was 90 or 200 ppb, pH ~ 8.1. EDTA was used at 92 ppm and polysaccharides at 0.001 wt%. Control samples without GA–PEI -DE particles are presented in bold text. (±) indicates S. D. between measurements (n=3).

1
2
3
4
5
6
7
8
9
10
11
12
13
14
15
16
17
18
19
20
21
22
23
24
25
26
27
28
29
30
31
32
33
34
35
36
37
38
39
40
41
42
43
44
45
46
47
48
49
50
51
52
53
54
55
56
57
58
59
60

Figure 1. Chemical structures of various polysaccharides considered in this study: (a) Lambda carrageenan; (b) Sodium alginate; and (c) Agarose.
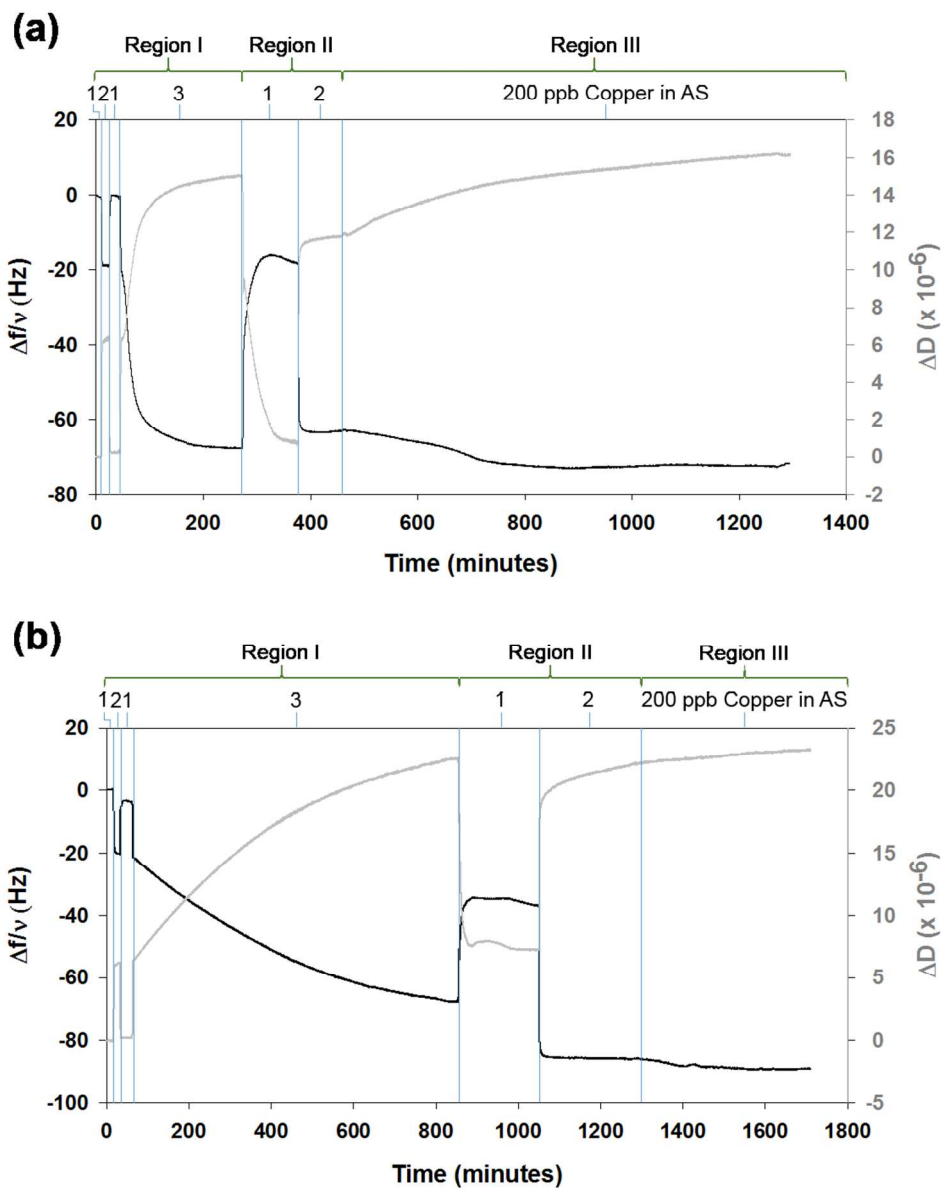Figure 1
78x36mm (300 x 300 DPI)

Figure 2. Representative QCM-D sensograms for adsorption and stability of (a) Carrageenan and (b) Alginate adsorbed onto the GA–PEI coatings from artificial seawater containing 0.001 wt% of the polysaccharide. Change in frequency (black) is given on the left Y-axis and dissipation (grey) is given on the right Y-axis. The vertical blue lines refer to the change of solution with 1 indicating Milli-Q water, 2 indicating artificial seawater (AS) and 3 indicating either (a) 0.001% carrageenan or (b) 0.001% alginate in artificial seawater. Region I includes establishment of baseline for GA–PEI in Milli-Q water 1 and artificial seawater 2, with subsequent adsorption of the polysaccharide (a) carrageenan and (b) alginate from artificial seawater 3, respectively. In Region II the stability of the adsorbed films was investigated upon reapplication of solutions 1 and 2. This was followed by copper uptake from 200 ppb in AS in Region III. The fifth overtones are graphed (F5 & D5).
Figure 2
95x119mm (300 x 300 DPI)

1
2
3
4
5
6
7
8
9
10
11
12
13
14
15
16
17
18
19
20
21
22
23
24
25
26
27
28
29
30
31
32
33
34
35
36
37
38
39
40
41
42
43
44
45
46
47
48
49
50
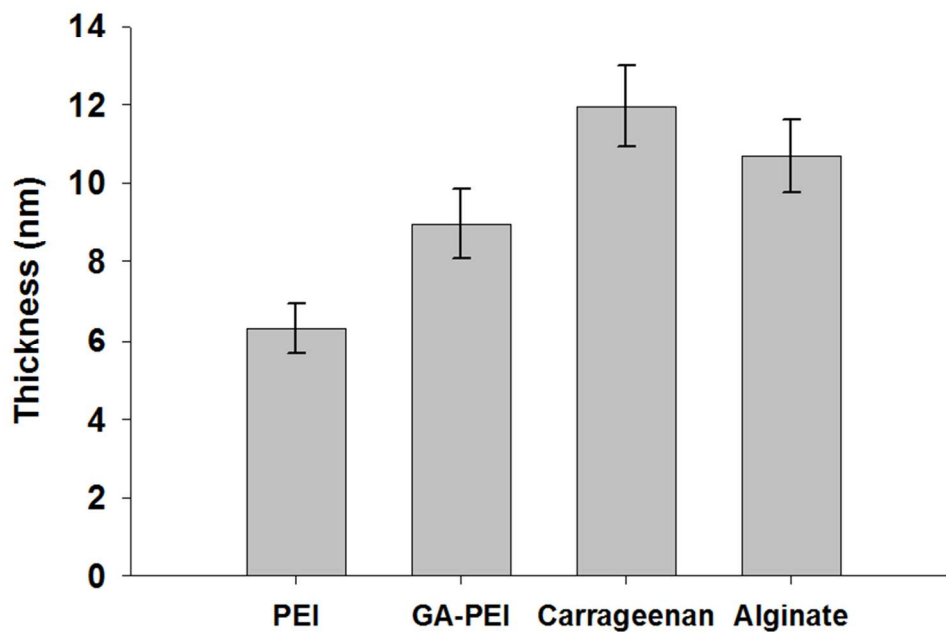51
52
53
54
55
56
57
58
59
60

Figure 3. Average thickness at different stages of the preparation process for GA–PEI coatings with an adsorbed layer of polysaccharide. Error bars indicate one standard deviation (n=54 and 22 for coatings with and without adsorbed polysaccharides, respectively.
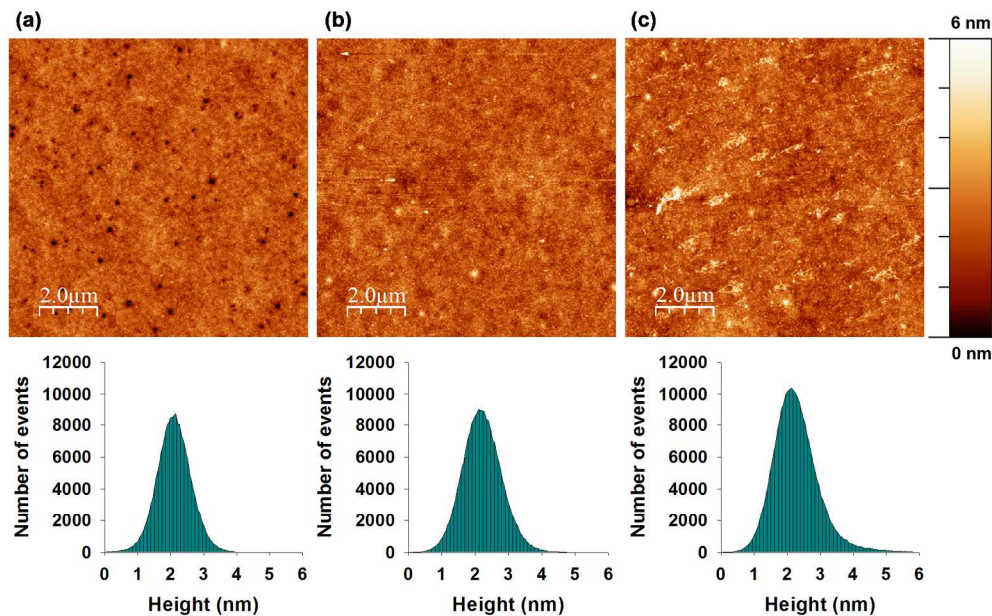Figure 3
72x59mm (300 x 300 DPI)

Figure 4. The top row presents AFM height images (10 x 10 µm2) of (a) PEI crosslinked with glutaraldehyde (GA–PEI) (b) Carrageenan on GA–PEI (c) Alginate on GA–PEI on a silicon wafer substrate. The small pinholes visible in (a) GA–PEI disappear after the adsorption of (b) Carrageenan or (c) Alginate The bottom row presents relative height histograms for the AFM topographic images respectively. Both (b) carrageenan and (9c) alginate covered surfaces presented a tail in the distribution towards higher structures, compared to bare (a) GA–PEI, with the tail being the most pronounced for alginate.
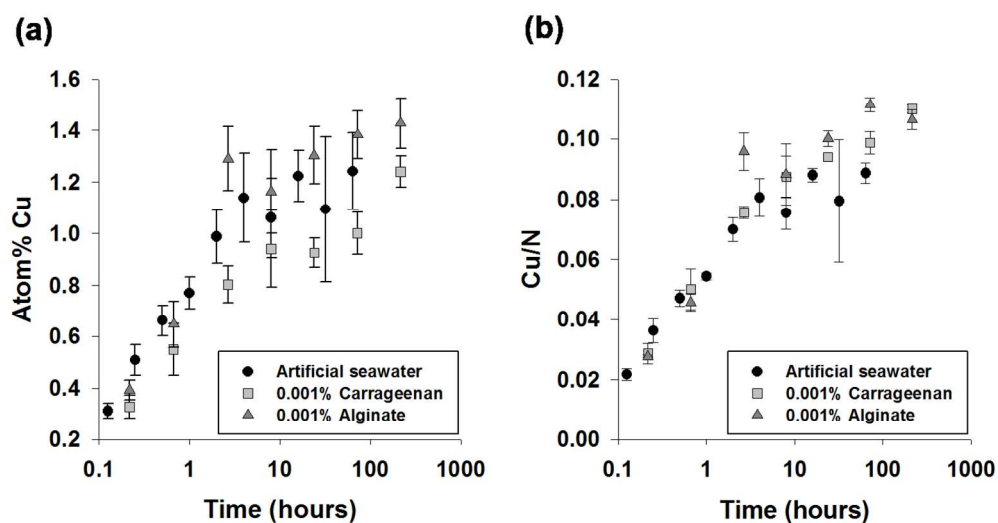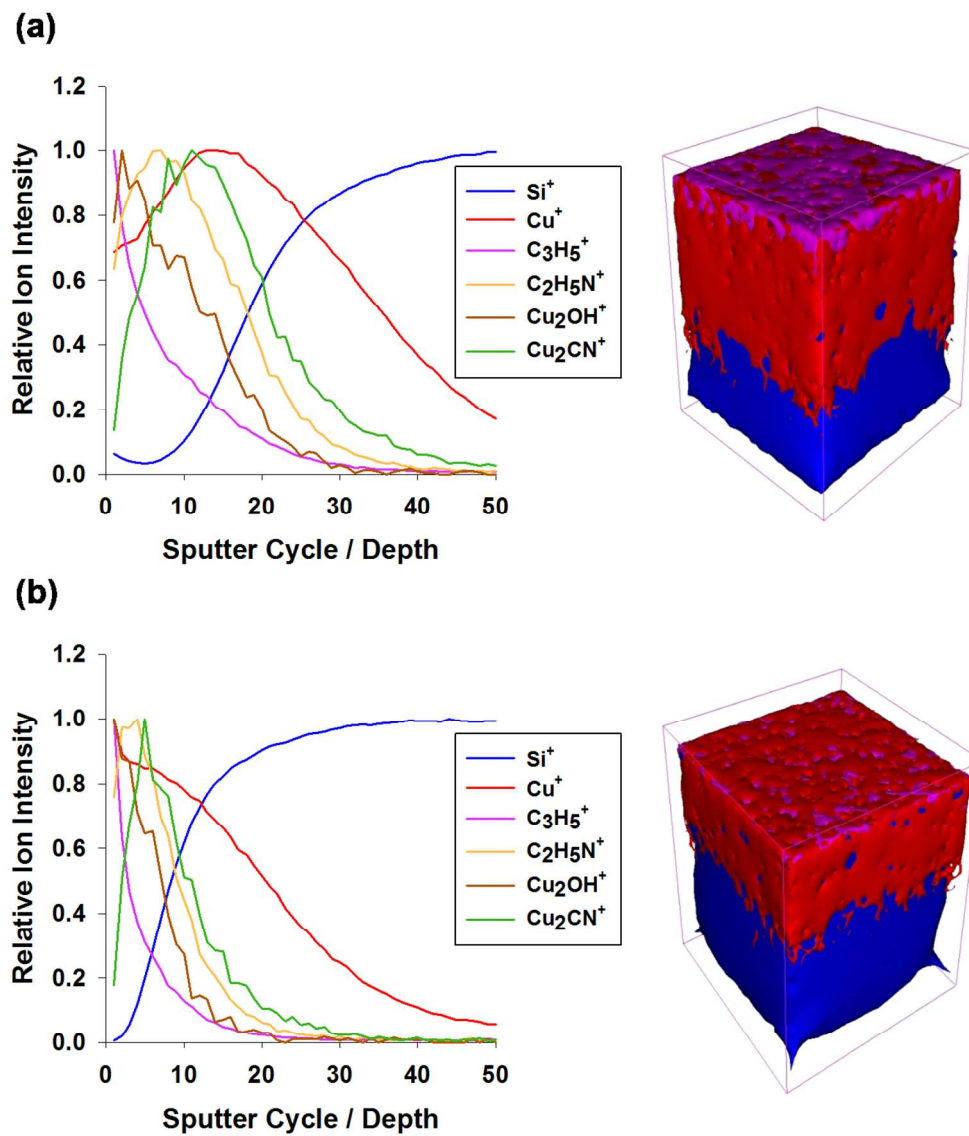
Figure 4
183x113mm (300 x 300 DPI)

Figure 5. Graphs showing (a) Atom% copper (Cu) and (b) Copper-to-nitrogen (Cu/N) ratio for GA–PEI coatings without adsorbed polysaccharides (●; circles), with adsorbed carrageenan (■; squares) and with adsorbed alginate (▲; triangles) after different immersion times in artificial seawater containing 200 ppb copper. Error bars indicate ± min/max (n = 2).
Figure 5
124x65mm (300 x 300 DPI)

1
2
3
4
5
6
7
8
9
10
11
12
13
14
15
16
17
18
19
20
21
22
23
24
25
26
27
28
29
30
31
32
33
34
35
36
37
38
39
40
41
42
43
44
45
46
47
48
49
50
51
52
53
54
55
56
57
58
59
60

(a)

(b)

Figure 6. Tof- SIMS depth profile through GA–PEI coatings adsorbed with (a) Carrageenan or (b) Alginate from 0.001% solution in artificial seawater. To the right are the corresponding 3D reconstruction of the Tof-SIMS depth profile presenting polysaccharide through C3H5+ fragment (pink) on a silicon substrate (blue) showing copper (red).
Figure 6
115x132mm (300 x 300 DPI)

1
2
3
4
5
6
7
8
9
10
11
12
13
14
15
16
17
18
19
20
21
22
23
24
25
26
27
28
29
30
31
32
33
34
35
36
37
38
39
40
41
42
43
44
45
46
47
48
49
50
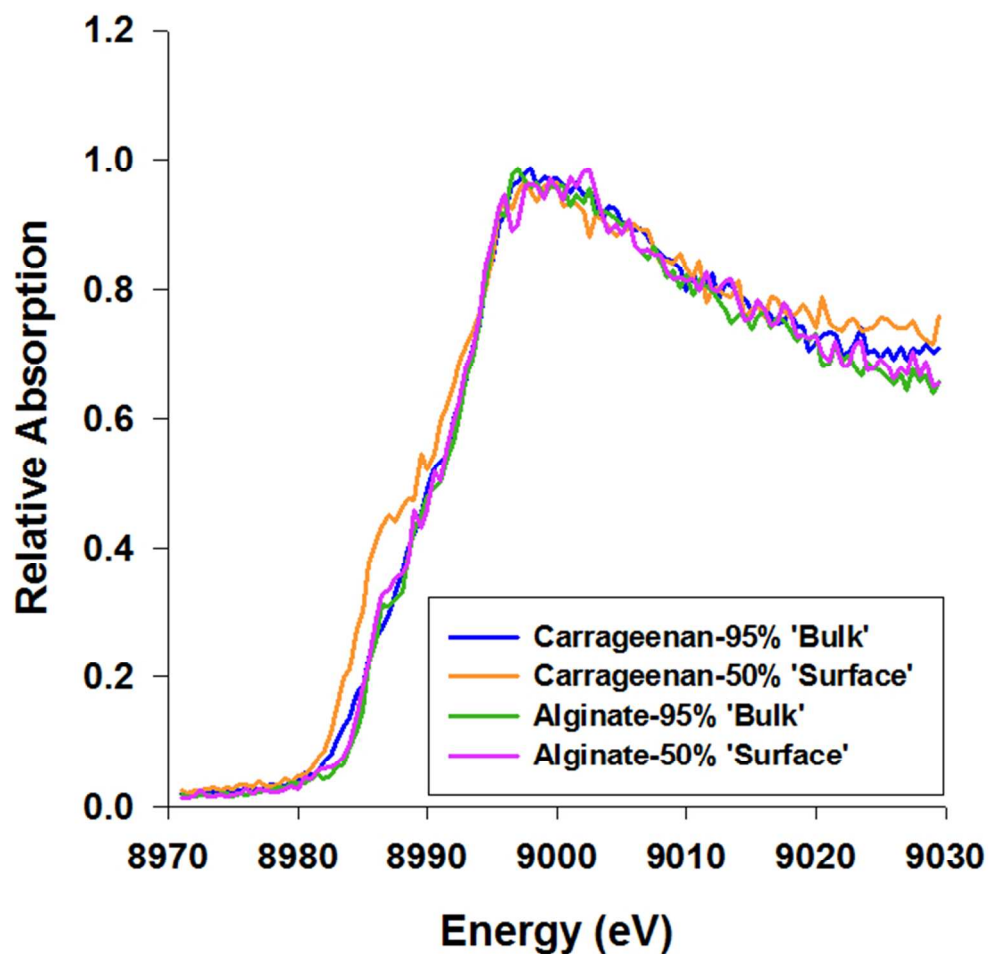51
52
53
54
55
56
57
58
59
60

Figure 7. Cu K-edge XANES spectra for copper; in GA–PEI adsorbed with carrageenan and GA–PEI adsorbed with alginate.
Figure 7
57x57mm (300 x 300 DPI)

1
2
3
4
5
6
7
8
9
10
11
12
13
14
15
16
17
18
19
20
21
22
23
24
25
26
27
28
29
30
31
32
33
34
35
36
37
38
39
40
41
42
43
44
45
46
47
48
49
50
51
52
53
54
55
56
57
58
59
60

Table 1

Sample	0.001 wt%	0.005 wt%	0.025 wt%
Carrageenan	+	+	+
Sodium alginate	+	+	-
Agarose	-	-	-

Table 2

Sample	[Cu] (ppb)
Artificial seawater	**200 ± 4.2**
GA–PEI–DE	≤ 10
GA–PEI–DE+ Alginate	≤ 10
GA–PEI–DE+ Carrageenan	≤ 10
GA–PEI–DE+ Alginate + Carrageenan	≤ 10
Artificial seawater + EDTA	**200 ± 1.9**
GA–PEI–DE	≤ 10
Artificial seawater + EDTA + Alginate + Carrageenan	**90 ± 1.2**
GA–PEI–DE+ EDTA + Alginate + Carrageenan	≤ 10

Supplementary Information

Unhindered copper uptake of glutaraldehyde-polyethyleneimine coatings in an artificial seawater model system with adsorbed swollen polysaccharides and competing ligand EDTA

Simarpreet Kaur[a], Ivan M. Kempson[a], Johan B. Lindén[a,1], Mikael Larsson[a,b*] and Magnus Nydén[a,b]

[a]*Future Industries Institute, University of South Australia, Mawson Lakes, South Australia 5095, Australia.*

[b]*School of Energy and Resources, University College London, 220 Victoria Square, Adelaide, South Australia 5000, Australia*

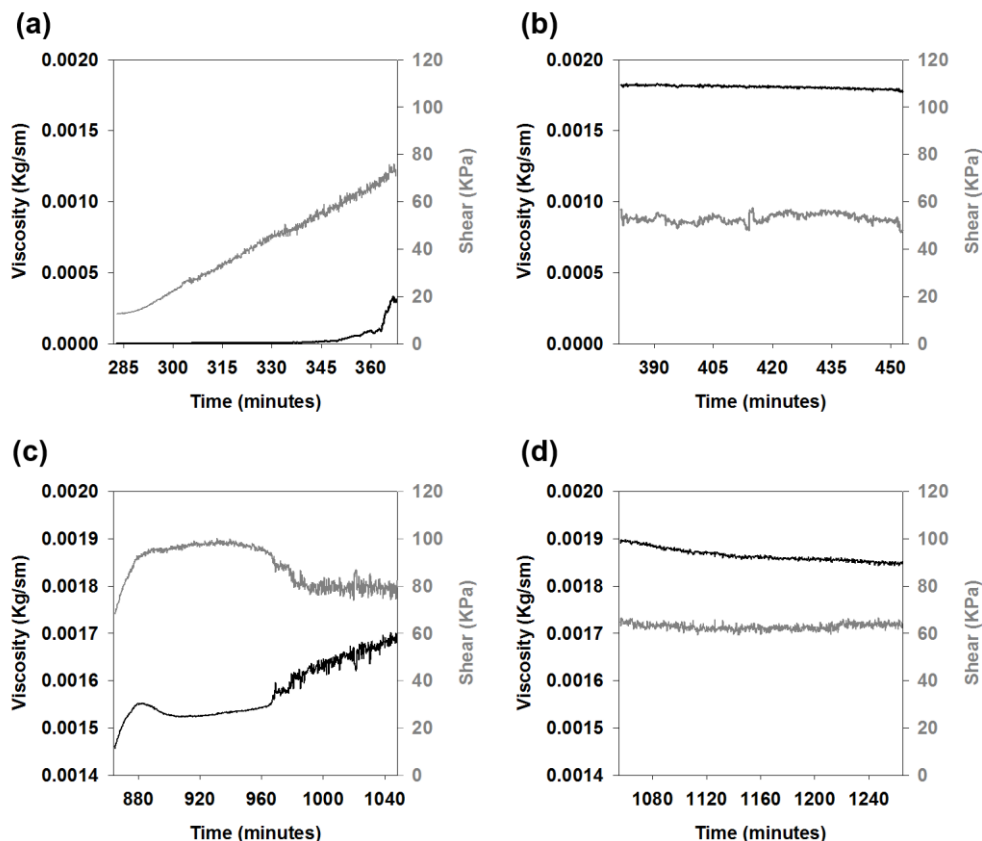*Corresponding author: E-mail: larsson.mikael@gmail.com

[1]Current address: SP technical research institute of Sweden, Brinellgatan 4, 504 62 Borås, Sweden

Table S1. Composition of the used artificial seawater, as per specification sheet (Sigma Aldrich, Specification: PRD.0.ZQ5.10000031869, product number: S9883, http://www.sigmaaldrich.com/Graphics/COfAInfo/SigmaSAPQM/SPEC/S9/S9883/S9883-BULK_____SIGMA____.pdf <accessed 2016-11-19>).

Ionic species present in sea salts	Concentration (ppm)
Chloride	19290
Sodium	10780
Sulfate	2660
Potassium	420
Calcium	400
Carbonate (Bicarbonate)	200
Strontium	8.8
Boron	5.6
Bromide	56
Iodide	0.24
Lithium	0.3
Fluoride	1.0
Magnesium	1320
Other trace elements	< 0.5

Table S2. Experimental and fitted Δf and ΔD values of the polysaccharide layers on GA-PEI coatings for the Region II after polysaccharide adsorption, as determined by extended viscoelastic modelling using Voigt model for a single layer system. Standard deviation was determined from quadruplicates.
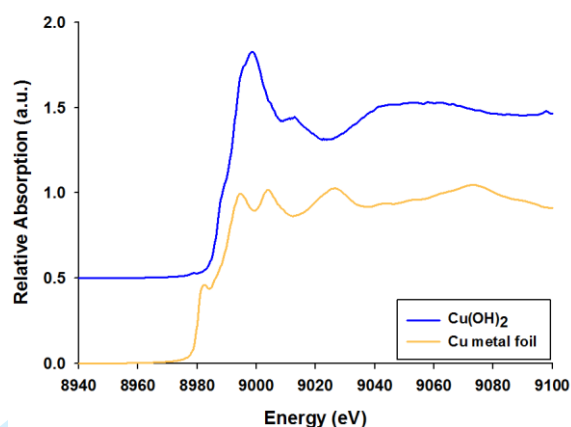
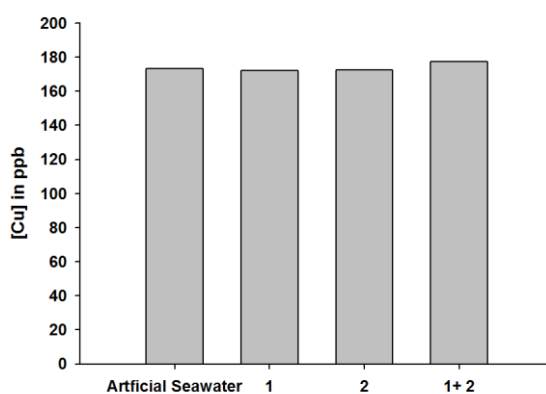|	Carrageenan		Alginate	
	Milli-Q water	*Artificial seawater*	*Milli-Q water*	*Artificial Seawater*
Experimental Δ F (Hz)	-18 ± 3.4	-63 ± 1.5	-39.2 ± 2.3	-87 ± 1.9
Fitted Δ F (Hz)	-18 ± 3.7	-61 ± 1.6	-39 ± 2.4	-87 ± 2.0
Experimental ΔD (x 10⁻⁶)	1.3 ± 0.3	12.4 ± 0.6	7.1 ± 0.8	21.6 ± 0.6
Fitted ΔD (x 10⁻⁶)	1.2 ± 0.3	12.1 ± 0.6	7 ± 0.8	21.6 ± 0.7

Figure S1. Modelled viscosity (black) and shear modulus (grey) after the adsorption of (a) Carrageenan in Milli-Q water, (b) Carrageenan in artificial seawater, (c) Alginate in Milli-Q water and (d) Alginate in artificial seawater.

Table S3. Hydrated thickness of the polysaccharide layers on *GA–PEI* coatings for the Region II after polysaccharide adsorption, as determined by extended viscoelastic modelling using Voigt model for a single layer system. Standard deviation was determined from quadruplicates.
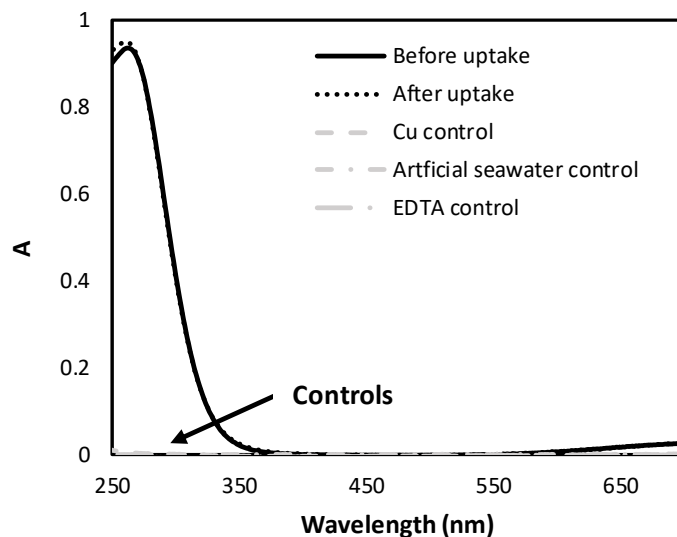
Polysaccharide	Modelled thickness (nm)	
	Milli-Q water	*Artificial Seawater*
Carrageenan	2.4 ± 0.5	21.4 ± 0.4
Alginate	12.8 ± 1.2	38.4 ± 0.7

Figure S2. Cu K-edges XANES showing copper hydroxide along with a reference foil (Cu metal foil) for energy calibration.

Figure S3. Copper concentration in control solutions after centrifugation, as determined through ICP-OES. The solutions included artificial seawater without polysaccharides and with 0.001% of carrageenan (1), alginate (2) and carrageenan and alginate (1+2).

Figure S4. UV-Vis spectroscopic analysis to determine if EDTA was bound and removed from solution by the GA–PEI–DE particles during the copper uptake procedure. Artificial seawater initially containing 92 ppm (0.31 mM) EDTA was subjected to the copper removal procedure using GA–PEI–DE. Copper was added at equimolar concentration to EDTA (0.31 mM) before (black solid line) or after (dotted black line) the copper uptake procedure and the UV-Vis spectra of formed EDTA-Cu complexes were recorded. Pure artificial seawater, seawater containing 92 ppm EDTA and Milli-Q water containing 0.31 mM copper concentration (since copper was not fully soluble in artificial seawater at the used concentration) were included as controls. No relevant difference in EDTA-Cu absorbance spectra was detected between samples before and after the uptake procedure, which proved that EDTA was not bound and removed from the solution by the GA–PEI–DE particles.